Role of the S2 and S3 Segment in Determining the Activation Kinetics in Kv2.1 Channels

R. Koopmann[1], **A. Scholle**[1], **J. Ludwig**[2,*], **T. Leicher**[2], **T. Zimmer**[1], **O. Pongs**[2], **K. Benndorf**[1]

[1]Institut für Physiologie, Herz-Kreislauf-Physiologie, Friedrich-Schiller-Universität, 07740 Jena, Germany
[2]Zentrum für Molekulare Neurobiologie, Institut für Neurale Signalverarbeitung, UKE (Haus 42), Martinistr. 52, 20251 Hamburg, Germany

Abstract. We constructed chimeras between the rapidly activating Kv1.2 channel and the slowly activating Kv2.1 channel in order to study to what extent sequence differences within the S1–S4 region contribute to the difference in activation kinetics. The channels were expressed in *Xenopus* oocytes and the currents were measured with a two-microelectrode voltage-clamp technique. Substitution of the S1–S4 region of Kv2.1 subunits by the ones of Kv1.2 resulted in chimeric channels which activated more rapidly than Kv2.1. Furthermore, activation kinetics were nearly voltage-independent in contrast to the pronounced voltage-dependent activation kinetics of both parent channels. Systematic screening of the S1–S4 region by the replacement of smaller protein parts resolved that the main functional changes generated by the S1–S4 substitution were generated by the S2 and the S3 segment. However, the effects of these segments were different: The S3 substitution reduced the effective gating charge and accelerated both a voltage-dependent and a voltage-independent component of the activation time course. In contrast, the S2 substitution accelerated predominantly the voltage-dependent component of the activation time course thereby leaving the effective gating charge unchanged. It is concluded that the S2 and the S3 segment determine the activation kinetics in a specific manner.

Key words: Kv2.1 and Kv1.2 channels — Activation time course — Voltage dependence — S2 and S3 transmembrane segments

* *Present address:* Department of Physiology II, Ob dem Himmelreich 7, 72074 Tübingen, Germany.

Correspondence to: K. Benndorf

Introduction

The α-subunits of voltage-dependent Kv-channels are integral membrane proteins that contain six membrane spanning regions (S1 to S6; Shih & Goldin, 1997). Four of these α-subunits assemble to constitute a functional channel (MacKinnon, 1991). Opening of Kv-channels is controlled by the transmembrane potential. This control is mediated by displacement of charge in a voltage sensor (Hodgkin & Huxley, 1952). The past years have brought important insights into identifying the regions that contribute to the voltage sensor and to the structural rearrangements underlying gating. One main element of the voltage sensor is the S4 segment (Liman et al., 1991; Papazian et al., 1991; Logothetis et al., 1992; Perozo et al., 1994; Larsson et al., 1996; Mannuzzu et al., 1996; Yusaf, Wray & Sivaprasadarao, 1996; Starace, Stefani & Bezanilla, 1997; Cha & Bezanilla, 1998). The amino-acid sequences of the S4 segments of Kv channels share a common motif of several basic amino acids at every third position $((K/R\text{-}x\text{-}y)_n)$. In *Shaker* channels it has been shown that only few positively charged amino-acids in S4 (R365, R368, R371) carry the main fraction of the gating charge (Aggarwal & MacKinnon, 1996; Seoh et al., 1996), quite in analogy to the structurally related voltage-dependent Na+ channels (for review *see* Horn, 2000). In *Shaker*, also an acidic residue in S2 (E293) contributes to the gating charge (Seoh et al., 1996). Other well-conserved acidic residues in the S2 and S3 sequences of Kv-channels were also proposed to contribute to voltage sensing by interacting electrostatically with some of the basic residues in the S4 segment (Papazian et al., 1995; Planells-Cases et al., 1995; Tiwari-Woodruff et al., 1997). A tryptophan-scanning analysis of the S2 segment has suggested that this segment has an α-helical structure (Monks, Needleman & Miller, 1999). The conserved acidic residues are located at one side of the helix. This side presumably interacts

with S4, while the other side may contribute to the lipid-exposed surface of the channel. An involvement of the S2 segment in the voltage-dependent gating has also been reported by Cha & Bezanilla (1997) in *Shaker* and by Milligan & Wray (2000) in Kv2.1 channels.

Recently, a model for *Shaker* channel activation has been described that is based on fluorescence resonance energy transfer measurements. In this model, gating charge movement mainly results from a twist of the S4 segment (Glauner et al., 1999; Cha et al., 1999). Moreover, structural rearrangements of the voltage sensor associated with activation may not only be influenced by S4, but also by other protein parts which are not directly linked to the gating-charge displacement. Since shifts in steady-state activation are often observed when mutating the transmembrane segments or regions even outside S1 to S6, it is likely that such regions are also involved in control of voltage-dependent activation.

Despite the growing insight into the function of the voltage sensor, only very little is known about the determinants of the time course of gating. It was suggested that the S3/S4 linker may distinctly influence the activation time course (Mathur et al., 1997). To systematically screen for structural determinants of the activation time course, we analyzed chimeras between two Kv-channels that are different in this respect, the slowly activating Kv2.1 and the rapidly activating Kv1.2. In these chimeras we substituted elements of Kv2.1 by the respective ones of Kv1.2. In a previous study we described the effects of substitutions within the S4–S6 region. These results identified the S4 segment, the S5/P linker and the deep pore to partly account for the slow activation of Kv2.1 compared to Kv1.2 (Scholle et al., 2000). Herein, we characterize domains in the S1 to S4 region that contribute to the slow activation of Kv2.1. We show that the S2 and the S3 segment are important structural elements to determine the activation time course of Kv2.1.

Materials and Methods

In Vitro Mutagenesis

Chimeric cDNAs between rat Kv1.2 (Acc. No. X16003) and human Kv2.1 (Acc. No. X68302) were obtained by overlap polymerase chain reactions (PCR; Ho et al., 1989). cDNAs were cloned into the pGEM-HE vector for RNA synthesis (Liman, Tytgat & Hess, 1992). For the different chimeras, fragments containing the nucleotides (nt) given below were fused together. Numbers refer to the open reading frame of the respective channel cDNAs.

	hKv2.1	rKv1.2	hKv2.1
CH_S1–S4	1–555	478–945	955–stop
CH_S1–S3	1–555	478–843	862–stop
CH_S1	1–555	478–550	627–stop
CH_L1/2	1–627	551–663	685–stop
CH_S2–S3	1–684	664–843	862–stop
CH_S2	1–684	664–735	757–stop
CH_L2/3	1–757	736–753	778–stop
CH_S3	1–777	754–843	862–stop
CH_L3/4–S4	1–840	820–945	955–stop

DNA sequences amplified by PCR were verified by sequencing using the BigDye terminator cycle sequencing kit (Perkin Elmer, Weiterstadt, Germany). Sequence reactions were analyzed on Prism 310 automated sequencer (Perkin Elmer).

Plasmid DNAs were linearized for cRNA synthesis, which was performed using a commercial kit (mMessage mMachine, Ambion, Austin, TX) and T7 polymerase. Denaturing agarose gel electrophoresis was used to check the quality of cRNA product of each reaction and to quantify the yield.

Oocyte Preparation

Ovarian lobes from *Xenopus laevis* where resected under anesthesia (0.3% 3-aminobenzoic acid ethyl ester) and transferred to a Petri dish containing Barth medium (mM: NaCl 84, KCl 1, NaHCO$_3$ 2.4, MgSO$_4$ 0.82, Ca(NO$_3$)$_2$ 0.33, CaCl$_2$ 0.41, Tris 7.5, pH = 7.4 with HCl). The oocytes were incubated in Ca^{2+}-free Barth medium containing 1–2 mg/ml collagenase (Type 1, Sigma, St. Louis, MO) for 1–2 hr. After washing repeatedly with Barth medium containing Ca^{2+} the oocytes were isolated and defolliculated mechanically. Within 6 hr after isolation the oocytes were injected with ~50 nl cRNA solution. The cRNA concentration was varied for control of the expression level. The oocytes were stored at 18 °C in Barth medium until experimental use within 3 days after injection.

Electrophysiology

Whole-cell currents were recorded with the two-microelectrode voltage-clamp technique using a commercial amplifier (OC725C, Warner Instrument). Glass electrodes were filled with 3 M KCl and they had a resistance of 0.3 to 0.7 MΩ. The experiments were performed in modified Barth medium containing 5 mM KCl and 80 mM NaCl. The experiments were controlled with the recording program of the ISO2 software (MFK, Niedernhausen, Germany). Currents were elicited from a holding potential of –80 mV (all channels but Ch_L1/2) or –120 mV (Ch_L1/2). The sampling rate was 5 kHz.

Steady-state activation was determined with a double-pulse protocol. After 500-msec prepulses to different test voltages, the voltage was clamped for 300 msec to 0 mV (pulsing frequency 0.1 Hz). Since at 0 mV activation and deactivation are slow compared to the decay of the capacitive transient, steady-state activation could be determined easily by evaluating the instantaneous current after the decay of the capacitive transient (1–3 msec after the beginning of the test pulse). The amplitudes of the instantaneous currents with respect to the maximum instantaneous current were plotted as function of voltage (*see* Fig. 1). Steady-state activation was determined by fits with the modified Boltzmann function

$$I = I_{max}/(1 + \exp(-(V - V_{1/2})/s)), \qquad (1)$$

yielding the midpoint voltage $V_{1/2}$ of half maximum channel activation and the slope factor s. We preferred to determine steady-state activation with conditioning pulses because the results are independent of possible differences in the driving force at different voltages and of possible permeability changes in the chimeras. One uncertainty associated with this procedure is that the degree of C-type inactivation during the prepulse is neglected. However, in the channels and chimeras tested, C-type inactivation during the prepulse was either absent
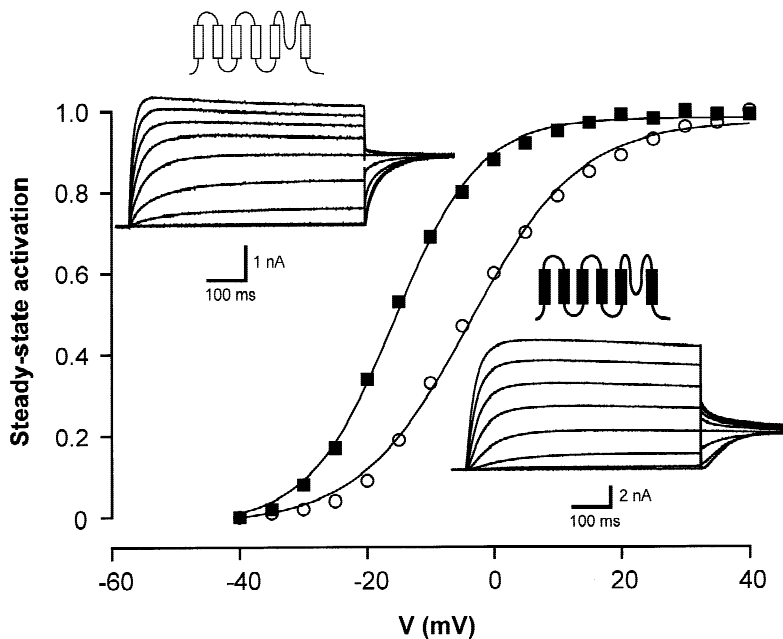
Fig. 1. Determination of steady-state activation. Original current recordings and the resulting steady-state activation curves. Prepulses of 500 msec duration were elicited to potentials between −40 and +40 mV in 5 mV increments. The prepulses were followed by test pulses of 300 msec to 0 mV. The insets show original current recordings (prepulse voltage 10 mV increments, test currents not shown until the end of the pulse). The current amplitude immediately after the capacitive transient (1–3 msec after the clamp step) was evaluated, normalized according to the maximum current I_{max}, and plotted as function of the voltage V of the prepulse. The data points were fitted with equation (*1*) yielding the slope parameter s and the voltage of half maximum activation $V_{1/2}$. The values are: Kv1.2, $V_{1/2} = -15.7$ mV, $s = 6.7$ mV; Kv2.1, $V_{1/2} = -3.8$ mV, $s = 8.7$ mV.

or of irrelevant amplitude. The speed of activation was determined by the time ($t_{a,1/2}$) at which the current was half of the peak current. This parameter was not corrected for the clamp speed.

STATISTICS

All values are given as mean ± SEM.

Results

STEADY-STATE ACTIVATION OF Kv2.1/Kv1.2 CHIMERAS

Heterologous expression of Kv2.1 channels in *Xenopus* oocytes gave rise to slowly activating, voltage-dependent outward currents with a voltage of half-maximum steady-state activation ($V_{1/2}$) of −3.5 ± 0.2 mV ($n = 102$). By contrast, the expression of Kv1.2 channels gave rise to rapidly-activating outward currents with a $V_{1/2}$ of −17.9 ± 0.5 mV ($n = 23$). Figure 1 shows examples of such currents for each of the wild-type channels. We constructed 9 chimeras between Kv2.1 and Kv1.2 to study the contributions of the S1–S4 region to the differences in Kv2.1 and Kv1.2 channel gating (Fig. 2). In the Table the chimeras Ch_S1–S4 to Ch_S3 were constructed by inserting either the complete S1–S4 region or part of it from Kv1.2 to Kv2.1. Each chimera expressed functional, voltage-dependent channels. The Table also summarizes the $V_{1/2}$ and s value obtained from the Boltzmann fits (equation *1*). In comparison to Kv2.1 currents, Ch_S1, Ch_L1/2 and Ch_S2 showed negative shifts in their steady-state activation with $V_{1/2}$ values of −20, −38 and −10 mV, respectively. On the

other hand, currents mediated by the four chimeras Ch_S1–S3, Ch_S2–S3, Ch_L2/3, and Ch_S3 activated at significantly more depolarized voltages than Kv2.1 currents ($V_{1/2}$ values between +7 and +26 mV). Ch_S1–S4 and Ch_L3/4–S4 gave rise to voltage-dependent currents with a $V_{1/2}$ close to that of Kv2.1. Thus, a transfer of the complete Kv1.2 S1–S4 region to Kv2.1 channels did not alter the $V_{1/2}$ value. This observation was unexpected because the segments S2 and S4 are viewed to be the voltage-sensing domains in *Shaker*-type Kv channels. By contrast, substitution of parts of the Kv2.1 S1–S4 region by respective Kv1.2 parts affected the voltage-dependence of steady-state activation of Kv2.1 currents.

REPLACING THE S1–S4 REGION IN Kv2.1 YIELDS A CHIMERA WITH A FAST AND LARGELY VOLTAGE-INDEPENDENT ACTIVATION TIME COURSE

As previously reported, Kv2.1-mediated currents activate slowly in response to stepwise depolarizations (Fig. 3, top; *see also* Benndorf et al., 1994). We quantified the activation time course at various voltages by the rise-time to the half-maximum current ($t_{a,1/2}$). We used this simple criterion because the rise-time can be easily obtained from current records and is independent of model assumptions. Furthermore, $t_{a,1/2}$ is presumably not significantly influenced by small slow components of activation and C-type inactivation. For Kv2.1-mediated currents (*Kv2.1* currents) the activation time course was strongly voltage dependent (Fig. 3, top). The value of $t_{a,1/2}$ was 76.0 ± 1.6 msec at −10 mV ($n = 117$) and 18.8 ± 0.4 msec at +40 mV ($n = 121$). Kv1.2 currents also
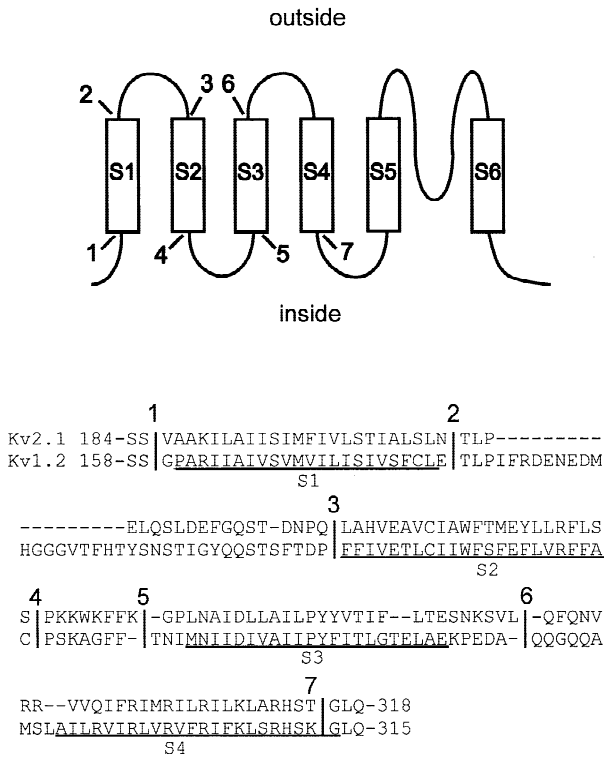
outside

inside

```
                    1                              2
Kv2.1 184-SS|VAAKILAIISIMFIVLSTIALSLN|TLP---------
Kv1.2 158-SS|GPARIIAIVSVMVILISIVSFCLF|TLPIFRDENEDM
             S1
                              3
---------ELQSLDEFGQST-DNPQ|LAHVEAVCIAWFTMEYLLRFLS
HGGGVTFHTYSNSTIGYQQSTSFTDP|FFIVETLCIIWFSFEFLVRFFA
                           S2
  4       5                                    6
S|PKKWKFFK|-GPLNAIDLLAILPYYVTIF--LTESNKSVL|-QFQNV
C|PSKAGFF-|TNIMNIIDIVAIIPYFITLGTELAEKPEDA-|QQGQQA
                           S3
                 7
RR--VVQIFRIMRILRILKLARHST|GLQ-318
MSLAILRVIRLVRVFRIFKLSRHSK|GLQ-315
           S4
```

Fig. 2. Alignment of the amino-acid sequence of Kv2.1 and Kv1.2 in the S1–S4 region. The numbers 1–7 indicate the positions used to link the protein parts in the chimeras. The graphic scheme at the top illustrates these positions according to the presently accepted channel topology.

showed a strongly voltage-dependent time course of activation in this voltage range but the time course was approximately threefold faster (Fig. 3, middle). The value of $t_{a,1/2}$ was 22.4 ± 2.0 msec at −10 mV (n = 22) and 4.8 ± 0.4 msec at +40 mV (n = 23). Ch_S1–S4 currents (Fig. 3, bottom) activated twofold faster than Kv2.1 currents at +40 mV ($t_{a,1/2}$ = 8.3 ± 0.3 msec, n = 10) and fourfold faster at −10 mV ($t_{a,1/2}$ = 16.4 ± 1.1 msec, n = 10). These results show that the activation time course of Ch_S1–S4 currents is less voltage-dependent than are the ones of Kv2.1 and Kv1.2 currents. Furthermore, the activation of Ch_S1–S4 currents at −10 mV was also faster than that of Kv1.2 currents at −10 mV. These data show that the S1–S4 region is an essential determinant for both the degree of voltage dependence and the rate of the activation time course of Kv2.1 currents.

To quantify the voltage dependence of the time course of activation, $t_{a,1/2}$ was plotted as function of the membrane voltage. Fig. 4 shows these plots for the wild type channels. Assuming an exclusively voltage-dependent process determining the speed of activation, the relationships were fitted with (dashed lines)

$$t_{a,1/2}(V) = t_1(V_{1/2})\exp(-q(V - V_{1/2})/kT). \qquad (2)$$

V is the membrane voltage, $t_1(V_{1/2})$ is $t_{a,1/2}$ at $V = V_{1/2}$, q the effective gating charge, k the Boltzmann constant, and T the temperature in Kelvin. The result is that equation 2 is inadequate to describe these data. We therefore tested to fit the $t_{a,1/2}$-voltage relationships by the sum of a voltage-dependent and a voltage-independent component

$$t_{a,1/2}(V) = t_1(V_{1/2})\exp(-q(V - V_{1/2})/kT) + t_2 \qquad (3)$$

with t_2 being the voltage-independent component. All other symbols have the same meaning as in equation 2. The result was that the $t_{a,1/2}$-voltage relationships were adequately described (continuous lines in Fig. 4). In our analysis we preferred to use $t_1(V_{1/2})$ as amplitude parameter instead of $t_1(0\text{ mV})$ to account for the observed differences in the $V_{1/2}$ values among the channels and chimeras. Equation 3 allowed us to quantify the voltage dependence of the effective gating charge q associated with $t_{a,1/2}$, independently of the $V_{1/2}$ value of each channel. The parameters obtained will be discussed together with those of the chimeras below.
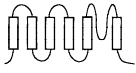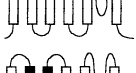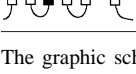
THE EFFECTS OF S1–S4 SUBSTITUTION CAN BE CONFINED TO S2 AND S3

In the following analysis we investigated the activation time course in chimeras in which parts of the S1–S4 region were exchanged. Similar to Ch_S1–S4, the time course of activation in Ch_S1–S3 was faster than that of Kv2.1 currents and only weakly voltage-dependent (Fig. 5). By contrast, Ch_L3/4–S4 generated voltage-dependent currents with an activation time course very similar to Kv2.1. These results suggested that the different activation time courses of Kv2.1 and Ch_S1–S4 were caused by domains in the S1–S3 region.

Previously it has been suggested that negative charges within the S2 and S3 transmembrane segments contribute to the channel's voltage sensor (Papazian et al., 1995; Planells-Cases et al., 1995; Seoh et al., 1996). Similarly, we observed that substitution of the S2–S3 region (Ch_S2–S3) sufficed to obtain an activation time course with weak voltage dependence as observed in Ch_S1–S4 and Ch_S1–S3 (Fig. 6). However, at +40 mV the time course of current activation ($t_{a,1/2}$ = 18.8 ± 1.2 mV; n = 11) was not accelerated compared to Kv2.1.

When we substituted the S1 segment only, the resulting chimera (Ch_S1) mediated currents that had a voltage dependence of the activation time course like wt Kv2.1 (Fig. 6). In contrast, in a chimera with substituted S1–S2 linker (Ch_L1/2) the activation time course was only weakly voltage dependent in the range between −10 and +40 mV. However, in Ch_L1/2 steady-state activation was largely shifted to more negative voltages ($V_{1/2}$ = −37.5 mV). Inspection of the activation time course

Table. Overview over the wild-type channels and the constructed chimeric channels

	Linking sites	Channel	$V_{1/2}$ (mV)	n	s (mV)
		Kv2.1	-3.5 ± 0.2	(102)	8.1 ± 0.3
		Kv1.2	-17.9 ± 0.5	(23)	5.9 ± 0.2
	1,7	Ch_S1–S4	-5.8 ± 1.0	(10)	15.7 ± 0.7
	1,6	Ch_S1–S3	-19.0 ± 0.9	(16)	15.6 ± 0.6
	6,7	Ch_L3/4–S4	-5.9 ± 1.0	(17)	10.4 ± 0.2
	1,2	Ch_S1	-20.2 ± 1.2	(15)	11.9 ± 0.3
	2,3	Ch_L1/2	-37.5 ± 1.6	(13)	14.0 ± 0.5
	3,6	Ch_S2–S3	-22.3 ± 0.4	(11)	13.0 ± 0.3
	3,4	Ch_S2	-9.8 ± 1.4	(14)	14.2 ± 0.5
	4,5	Ch_L2/3	7.3 ± 0.4	(22)	10.6 ± 0.2
	5,6	Ch_S3	26.2 ± 1.2	(20)	14.2 ± 0.3

The graphic schemes each contain six boxes, which symbolize the transmembrane regions S1–S6, and curved lines, which symbolize the termini, the linker between the transmembrane regions, and the pure loop. Sequences of Kv2.1 are drawn as open boxes and thin lines, whereas sequences of Kv1.2 are drawn as black boxes and thick lines. The indicated channel names are used throughout the text. For the chimeras, the linking sites are indicated according to Fig. 2. The two columns on the right provide the values of $V_{1/2}$ and s as obtained from fitting with equation 1 based on n experiments.

at voltages near $V_{1/2}$ showed a strong voltage dependence of $t_{a,1/2}$. Most likely, the apparent weak voltage dependence between −10 mV and +40 mV is due to the shift in steady-state activation and not to a reduced voltage dependence of the activation time course per se. In conclusion, the weak voltage dependence of the Ch_S1–S3 current activation can be confined to the S2–S3 region.

We further analyzed the role of the individual structural elements within the S2–S3 region by constructing chimeras in which each particular element was substituted (Ch_S2, Ch_L2/3, Ch_S3). Substitution of the S2 segment alone yielded a chimera with a faster current activation at all voltages compared to Ch_S2–S3 and a weakly voltage-dependent $t_{a,1/2}$ (Fig. 7). Substitution of the S3 segment alone also reduced the voltage dependence of the activation time course. In contrast to the chimeras with substituted S2 or S3 transmembrane segments, substitution of the linker between S2 and S3

(Ch_ L2/3) did not influence the time course of current activation.

S2 AND S3 SUBSTITUTION AFFECT THE Kv2.1 ACTIVATION TIME COURSE DIFFERENTLY

To further analyze the differences in the $t_{a,1/2}(V)$ relationships of the various channels, we compared the parameters obtained from the fits of equation *3* to the data (Fig. 8). The results of the fits (lines in Figs. 4 to 7) showed that equation *3* was suitable for a quantitative description of the $t_{1/2}(V)$ relationships for all channels tested. Inspection of the three parameters ($t_1(V_{1/2})$, q, t_2) for the various chimeras yielded that in one group of the chimeras (group I: Ch_S1, Ch_L1/2, Ch_L2/3, Ch_L3/4–S4) the activation time course was roughly similar to that in Kv2.1. In a second group (group II: Ch_S1–S4,
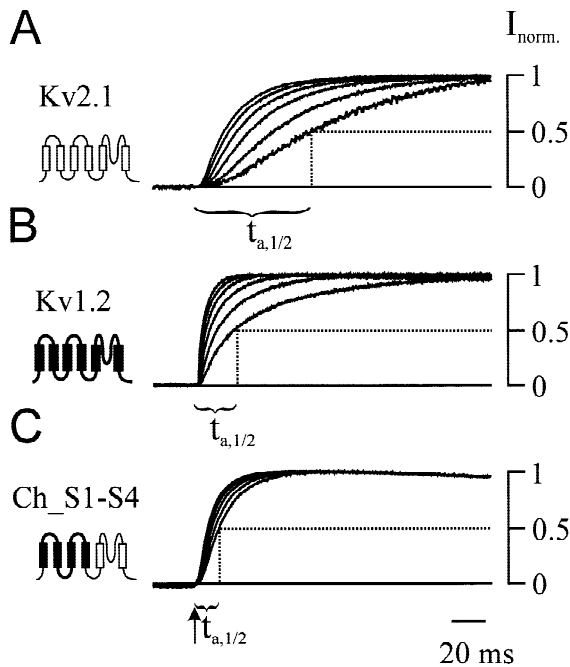
A

B

C

Fig. 3. Activation kinetics of Kv2.1, Kv1.2 and Ch_S1–S4 channels. The currents were elicited with test pulses to voltages between −10 and +40 mV and normalized with respect to the maximum current during the test pulse. At equal voltages Kv2.1 activates more slowly than Kv1.2. In contrast to the activation kinetics of the parent channels, those in Ch_S1–S4 are substantially less voltage dependent. Activation kinetics were quantified by the rise-time to half maximum current ($t_{a,1/2}$), measured from the beginning of the test pulse (*arrow*).

Ch_S1–S3, Ch_S2–S3, Ch_S3), the activation time course was different from that of Kv2.1 in two respects: the voltage-dependent component was less voltage-dependent (smaller q) and both, $t_1(V_{1/2})$ and t_2 were faster. In two chimeras (Ch_S1–S3 and Ch_S2–S3), t_2 approximated 0 ms, the reasonable low border for t_2. Since in the chimeras of group II the effective gating charge was reduced as compared to both parent channels, these results indicate a generally altered function of the voltage sensor. One chimera (group III: Ch_S2) cannot be attributed to group I or II. In this chimera, the main difference to Kv2.1 was a smaller value of $t_1(V_{1/2})$, whereas q was only slightly reduced as compared to the parent channels. This means that the apparently weak voltage dependence of $t_{a,1/2}$ in Ch_S2 may be caused mainly by a left shift of the $t_{a,1/2}(V)$ curve along the voltage axis with respect to that of Kv2.1. It is noteworthy that this shift was larger than the differences in the $V_{1/2}$ values of Ch_S2 and Kv2.1.

Discussion

The activation time course of both, Kv2.1 and Kv1.2 currents is voltage-dependent between −10 and +40 mV.

Activation is approximately three-fold faster in Kv1.2 than in Kv2.1 currents. In this study, we focused on the role of the S1–S4 region in the activation of Kv2.1 currents by constructing chimeras in which various sequences of Kv2.1 were substituted by the respective sequences of Kv1.2. We characterized steady-state activation and the voltage dependence of the activation time course for the currents mediated by these chimeras. In agreement with the present view, that gating is a cooperative process involving coordinated structural changes in several regions of the channel, we have shown that multiple substitution of structural elements in the S1–S4 region distinctly modified the gating in Kv2.1 channels: Transfer of the complete S1–S4 region of Kv1.2 into Kv2.1 accelerated activation. Unexpectedly, and in contrast to both parent channels, this chimera produced currents showing only a small voltage dependence of the activation time course. Transferring parts of the Kv1.2 S1–S4 region to Kv2.1 sufficed to induce a reduced voltage dependence of the activation time course. In particular, a pronounced reduction in the voltage dependence of the activation time course was observed for currents mediated by Kv2.1 chimeras containing either the S2 or the S3 transmembrane segment of Kv1.2 alone.

STEADY-STATE ACTIVATION OF CHIMERIC CHANNELS

Steady-state activation varied considerably among the currents generated by the different chimeras. As compared to Kv2.1, $V_{1/2}$ was shifted by more than 10 mV towards negative voltages in Ch_S1 and Ch_L1/2, and by more than 10 mV towards positive voltages in Ch_S1–S3, Ch_S2–S3, Ch_S3. In a preceding study we investigated chimeras between Kv1.2 and Kv2.1 with substitutions in the S4–S6 region (Scholle et al., 2000). We found that the $V_{1/2}$ values were shifted by more than 10 mV to positive potentials when substituting S4–S6 or only S4 and by more than 10 mV to negative potentials when substituting S6. Taken together, these results suggest that transfer of regions from Kv1.2 to Kv2.1 changes the relative stability of open and closed states of Kv2.1 channels such that transfer of domains between L2/3 and the P-region tend to destabilize the open state(s), whereas substitutions between S1 and S2 as well as S6 tend to stabilize the open state(s).

A change in the stability of the open conformation may arise from an altered interaction of the voltage sensor and the pore domain (S5–S6). The relevance of such an interaction for channel gating has been investigated by Li-Smerin, Hackos & Swartz, (2000) using tryptophan-scanning mutagenesis and analyzing the perturbations in gating energetics induced by the mutations. These authors proposed an interaction surface between the voltage sensor and the pore domain of *Shaker* channels. It is likely that the control of gating by an interac-
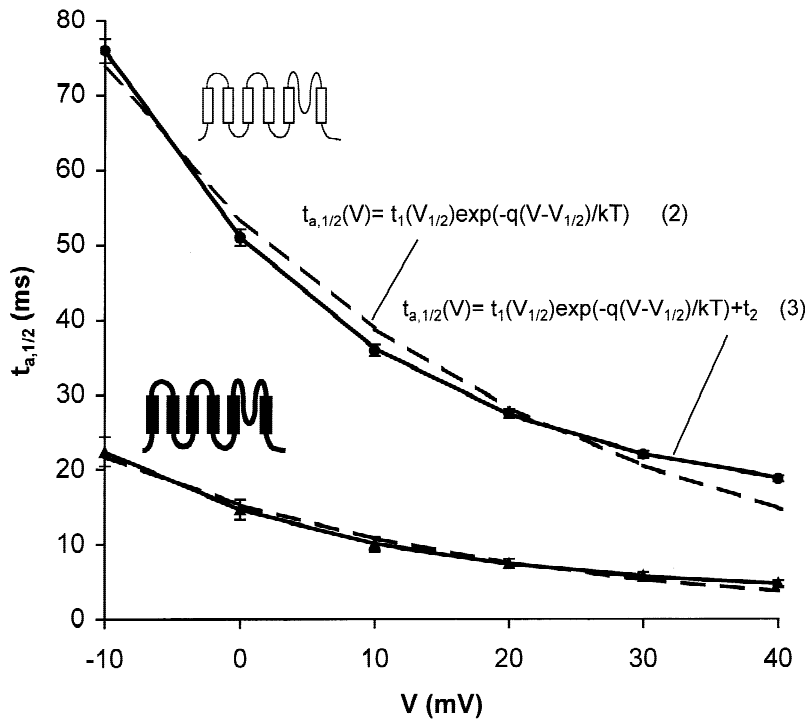
$$t_{a,1/2}(V) = t_1(V_{1/2})exp(-q(V-V_{1/2})/kT) \quad (2)$$

$$t_{a,1/2}(V) = t_1(V_{1/2})exp(-q(V-V_{1/2})/kT)+t_2 \quad (3)$$

Fig. 4. Activation kinetics ($t_{a,1/2}$) as function of voltage in Kv2.1 and Kv1.2. The dashed lines show the best fit with a voltage-dependent component only (equation 2). The data of Kv1.2 are described more adequately than those of Kv2.1. The continuous lines show the best fit with the sum of a voltage-dependent and a voltage-independent component (equation 3). Both relationships are described adequately. For meaning of the symbols in the equations *see* text.
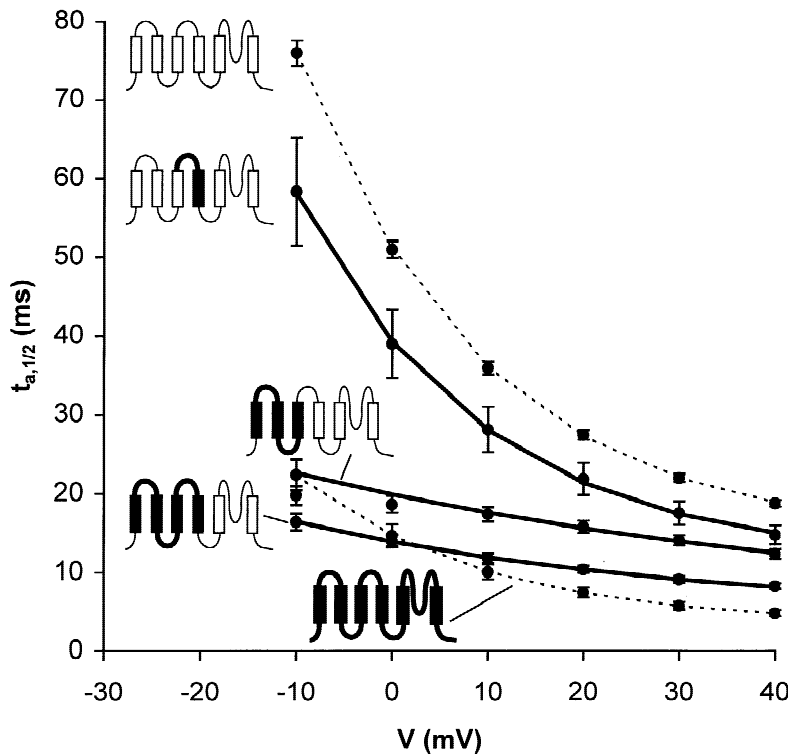

Fig. 5. Activation kinetics ($t_{a,1/2}$) as function of voltage in Kv2.1, Kv1.2, Ch_S1–S4, Ch_S1–S3 and Ch_L3/4–S4. Substitution of the S1–S3 region is sufficient to constitute a weakly voltage-dependent activation time course. Here and in the following diagrams, the lines represent the fits to the data with equation 3. Stippled lines indicate fits to data from wild-type channels already shown in Fig. 4.

tion-surface between pore domain and voltage-sensor is a general feature of voltage-gated K$^+$ channels. Changes in the interaction surface may at least in part account for the shifts in $V_{1/2}$ observed for currents mediated by the S5- and S6-Kv1.2/Kv2.1-chimeras (Scholle et al., 2000). Likewise, a modification of the interaction surface on the voltage sensor might contribute to the shift of $V_{1/2}$ in the chimera-mediated currents presented herein.
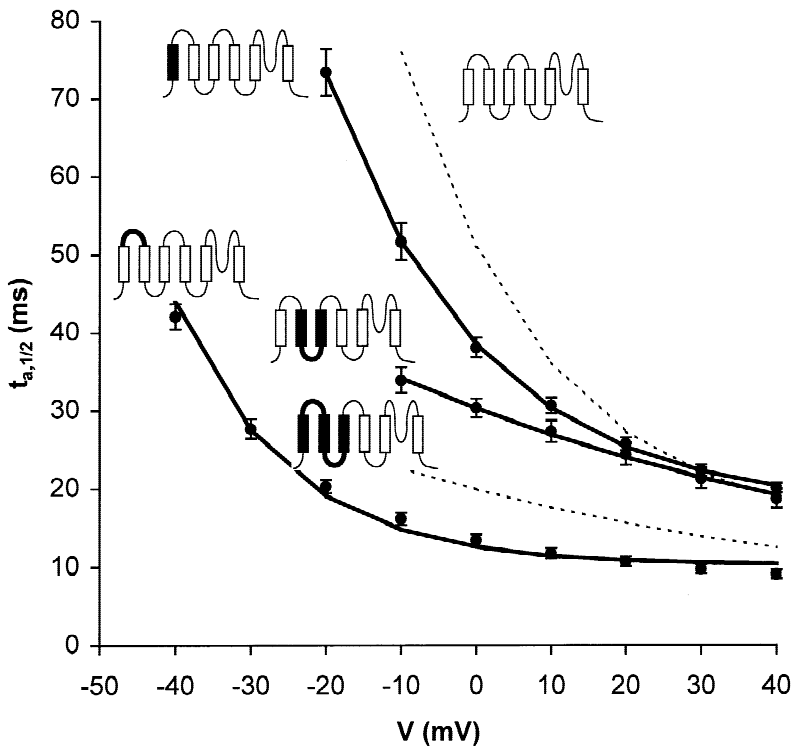
Fig. 6. Activation kinetics ($t_{a,1/2}$) as function of voltage in Ch_S1, Ch_L1/2 and Ch_S2–S3. Substitution of the S2–S3 region, but not of S1 or L1/2 induces an activation time course with only a weak voltage dependence. Activation kinetics as function of voltage in Kv2.1 and Ch_S1–S3 are plotted for comparison (stippled lines).
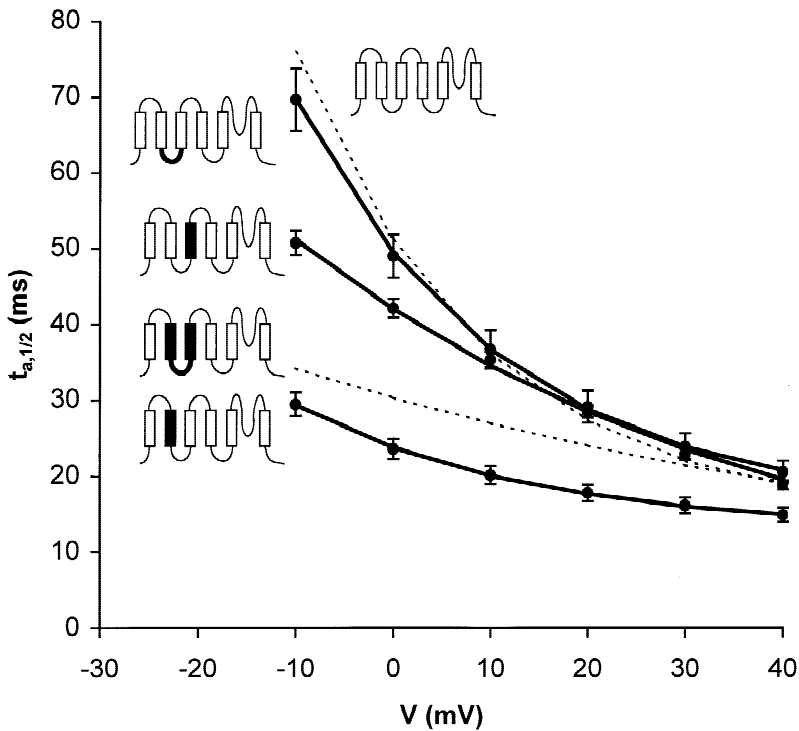

Fig. 7. Activation kinetics ($t_{a,1/2}$) as function of voltage in Ch_S2, Ch_L2/3 and Ch_S3. Activation kinetics in both, Ch_S2 and Ch_S3, are less voltage-dependent than those of Kv2.1.

Assuming the transmembrane topology proposed for the *Shaker* channel by Durell, Hao & Guy, (1998), the multiple regions within the S1–S6 primary structure causing negative or positive shifts of $V_{1/2}$ correspond to separate regions within the tertiary structure. This model proposes that hydrophilic side chains from S1–S3 and S6 line the gating pore. Altered interactions of these side-chains with the S4 segment in the activated or deacti-
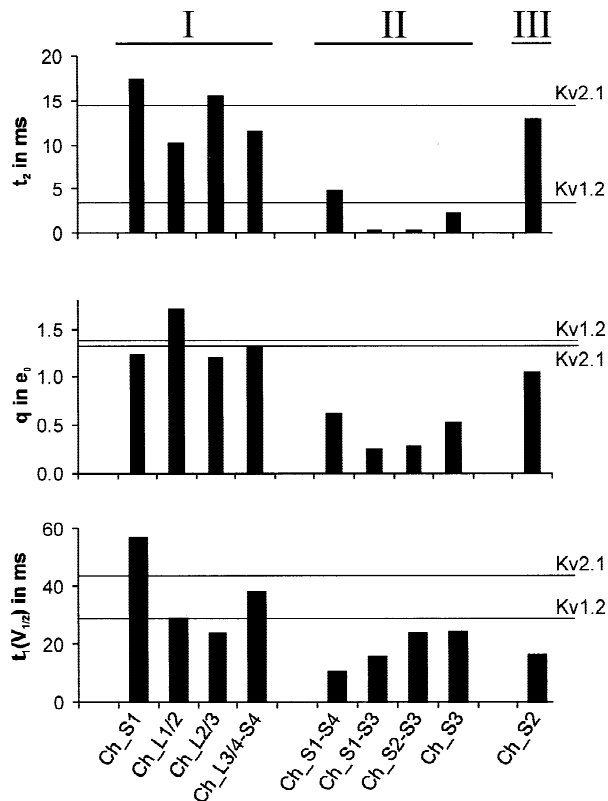
Fig. 8. Parameters as obtained from fitting equation *3* to the data of the various chimeras. The continuous and stippled lines indicate the parameters for Kv2.1 and Kv1.2, respectively. In the chimeras of group I, activation kinetics are similar to Kv2.1. In the chimeras of group II, q is reduced with respect to both parent channels. $t_1(V_{1/2})$ and t_2 are both shorter than in Kv2.1. Ch_S2 cannot be assigned to either group I or II. In this chimera (group III), q is only slightly reduced and t_2 is similar to Kv2.1.

vated position may produce the observed effects on the stability of the open conformation. Assuming that in chimeric constructs stabilizing interactions are more likely being impaired than strengthened, we propose that the S1–S2 and the S6 region in Kv2.1 are involved in interactions that stabilize the closed state (e.g., interactions with the S4 in the deactivated position). Accordingly, domains between S3 and the P-region are likely to form interactions that stabilize the open state (e.g., interactions with the S4 in the activated position).

With respect to the slope *s* of the steady-state activation curves, it was less steep (*s* was larger) in all chimeras compared to both wild type channels. This finding might indicate a reduced gating charge. However, also alterations in voltage-independent reactions of the activation might reduce the slope of steady-state activation, precluding a direct quantitative interpretation of the slope factor in terms of gating charges. When comparing the sequence of both wild-type channels (Fig. 2), the number of negative charges in S2 and S3 is equal,

whereas there are two extra positive charges in S4 of Kv1.2 (the first and the last arginine). To what extent these two charges contribute to the smaller slope factor in Kv1.2, and are thus positioned in the electric field, cannot be decided from our measurements because channels without this charge difference in S4 do also show very different slope factors (e.g., Kv2.1 versus Ch_L3/4–S4).

VOLTAGE DEPENDENCE OF THE ACTIVATION TIME COURSE

In some chimeras the voltage dependence of the activation time course was markedly attenuated. This effect was most prominent in Ch_S1–S4 and it could be confined mainly to the S2 and the S3 segment. In an attempt to differentiate for each chimera whether changed activation properties result from alterations of either less or more voltage-dependent transitions, we fitted equation *3* to the $t_{a,1/2}(V)$-curves. The results showed that the $t_{a,1/2}$-voltage relations for the parent channels and all the chimeras could be well described by this equation (lines in Figs. 5 to 7). This applicability may result from an activation process in which a more voltage-dependent step (or possibly more than one) limits the rate of activation at moderate depolarizations, while a less voltage-dependent step (or possibly more than one) limits the rate of activation at stronger depolarizations. The results suggest that the S2 and the S3 substitutions differently alter Kv2.1 activation (Fig. 8). The alteration in the activation kinetics by introducing the S2 segment of Kv1.2 into that of Kv2.1(Ch_S2) may lead to an acceleration of the voltage-dependent component. This is sufficient to account for the observed smaller voltage dependence. In contrast, the alterations introduced by the S3 substitution are more complex and affect both, voltage-dependent and voltage-independent components.

The combination of a faster activation than in Kv2.1 and a lesser voltage dependence than in both of the parent channels, as e.g., observed in Ch_S1–S4, might find an alternative explanation: The major component of the voltage-dependent gating might have shifted to more hyperpolarized voltages, so that at the holding voltage of most of the voltage sensors are nearly activated. If the final, less voltage-dependent, and not rate-limiting steps leading to the opening of the pore occur in the normal voltage range, this would result in both a faster activation kinetics and a decreased voltage dependence. Measurement of gating currents would be necessary for further addressing this problem.

IMPLICATIONS FOR THE GATING MECHANISM

Our results suggest that the S2 and S3 transmembrane segments in Kv2.1 channels contribute to the voltage

sensor. This finding is consistent with the present ideas for the role of S2 and S3 in *Shaker* channel gating. In this channel, it has been shown that an acidic residue in S2 (E293) contributes to the gating charge (Seoh et al., 1996) and further acidic residues in S2 and S3 were proposed to contribute to voltage sensing by interacting electrostatically with some of the basic residues in the S4 segment (Papazian et al., 1995; Planells-Cases et al., 1995; Tiwari-Woodruff et al., 1997). It is worth emphasizing that substitution of the S2 or the S3 segment changes the activation time course more severely than substitution of the S4 segment (Scholle et al., 2000). This finding might indicate that the different dynamics of the voltage sensor in Kv2.1 and Kv1.2 is mainly due to differences in the structures lining the gating pore than to differences in the S4 segment itself.

For *Shaker* channels, an activation model was proposed in which each of the four subunits undergoes at least two conformational changes, a strongly voltage-dependent and a weakly voltage-dependent conformational change (Zagotta, Hoshi & Aldrich, 1994). Assuming that the activation process of *Shaker* is generally valid for activation of Kv channels, our results support the idea that distinct structural elements may be attributed to these two conformational changes. The S3 segment may be a determinant of the voltage-independent (or less voltage-dependent) component. However, substitution of the S3 segment also reduces the effective charge of the voltage-dependent component as compared to both parent channels. This might indicate an impaired function of the voltage sensor. Substitution of the S2 segment has only a minor effect on the voltage-independent component and on the effective charge of the voltage-dependent component, but changes the amplitude of the voltage-dependent component. This result indicates an exclusive influence on the dynamics of the voltage-dependent component.

References

Aggarwal, S.K., MacKinnon, R. 1996. Contribution of the S4 segment to gating charge in the Shaker K$^+$ channel. *Neuron* **16**:1169–77

Benndorf, K., Koppmann, R., Lorra, C., Pongs, O. 1994. Gating and conductance properties of a human delayed rectifier K$^+$ channel expressed in frog oocytes. *J. Physiol.* **477**:1–14

Cha, A., Bezanilla, F. 1997. Characterizing voltage-dependent conformational changes in the *Shaker* K$^+$ channel with fluorescence. *Neuron* **19**:1127–1140

Cha, A., Bezanilla, F. 1998. Structural implications of fluorescence quenching in the Shaker K$^+$ channel. *J. Gen. Physiol.* **112**:391–408

Cha, A., Snyder, G.E., Selvin, P.R., Bezanilla, F. 1999. Atomic scale movement of the voltage-sensing region in a potassium channel measured via spectroscopy. *Nature* **402**:809–813

Durell, S.R., Hao, Y., Guy, H.R. 1998. Structural models of the transmembrane region of voltage-gated and other K$^+$ channels in open, closed, and inactivated conformations. *J. Struct. Biol.* **121**:263–284

Glauner, K.S., Mannuzzu, L.M., Gandhi, C.S., Isacoff, E.Y. 1999. Spectroscopic mapping of voltage sensor movement in the Shaker potassium channel. *Nature* **402**:813–817

Ho, S.N., Hunt, H.D., Horton, R.M., Pullen, J.K., Pease, L.R. 1989. Site-directed mutagenesis by overlap extension using the polymerase chain reaction. *Gene* **77**:51–59

Hodgkin, A.L., Huxley, A.F. 1952. A quantitative description of the membrane current and its application to conduction and excitation in nerve. *J. Physiol.* **117**:500–544

Horn, R. 2000. A new twist in the saga of charge movement in voltage-dependent ion channels. *Neuron* **25**:511–514

Larsson, H.P., Baker, O.S., Dhillon, D.S., Isacoff, E.Y. 1996. Transmembrane movement of the shaker K$^+$ channel S4. *Neuron* **16**:387–397

Liman, E.R., Hess, P., Weaver, F., Koren, G. 1991. Voltage-sensing residues in the S4 region of a mammalian K$^+$ channel. *Nature* **353**:752–756

Liman, E.R., Tytgat, J., Hess, P. 1992. Subunit stoichiometry of a mammalian K$^+$ channel determined by construction of multimeric cDNAs. *Neuron* **9**:861–871

Li-Smerin, Y., Hackos, D.H., Swartz, K.J. 2000. A localized interaction surface for voltage-sensing domains on the pore domain of a K$^+$ channel. *Neuron* **25**:411–423

Logothetis, D.E., Movahedi, S., Satler, C., Lindpaintner, K., Nadal Ginard, B. 1992. Incremental reductions of positive charge within the S4 region of a voltage-gated K$^+$ channel result in corresponding decreases in gating charge. *Neuron* **8**:531–540

MacKinnon, R. 1991. Determination of the subunit stoichiometry of a voltage-activated potassium channel. *Nature* **350**:232–235

Mannuzzu, L.M., Moronne, M.M., Isacoff, E.Y. 1996. Direct physical measure of conformational rearrangement underlying potassium channel gating. *Science* **271**:213–216

Mathur, R., Zheng, J., Yan, Y., Sigworth, F.J. 1997. Role of the S3–S4 linker in Shaker potassium channel activation. *J. Gen. Physiol.* **109**:191–199

Milligan, C.J., Wray, D. 2000. Local movement in the S2 region of the voltage-gated potassium channel hKv2.1 studied using cysteine mutagenesis. *Biophys. J.* **78**:1852–1861

Monks, S.A., Needleman, D.J., Miller, C. 1999. Helical structure and packing orientation of the S2 segment in the Shaker K$^+$ channel. *J. Gen. Physiol.* **113**:415–423

Papazian, D.M., Shao, X.M., Seoh, S.A., Mock, A.F., Huang, Y., Wainstock, D.H. 1995. Electrostatic interactions of S4 voltage sensor in Shaker K$^+$ channel. *Neuron* **14**:1293–1301

Papazian, D.M., Timpe, L.C., Jan, Y.N., Jan, L.Y. 1991. Alteration of voltage-dependence of Shaker potassium channel by mutations in the S4 sequence. *Nature* **349**:305–310

Perozo, E., Santacruz Toloza, L., Stefani, E., Bezanilla, F., Papazian, D.M. 1994. S4 mutations alter gating currents of Shaker K channels. *Biophys. J.* **66**:345–354

Planells-Cases, R., Ferrer Montiel, A.V., Patten, C.D., Montal, M. 1995. Mutation of conserved negatively charged residues in the S2 and S3 transmembrane segments of a mammalian K$^+$ channel selectively modulates channel gating. *Proc. Natl. Acad. Sci. U.S.A.* **92**:9422–9426

Scholle, A., Koopmann, R., Leicher, T., Ludwig, J., Pongs, O, Benndorf, K. 2000. Structural elements determining activation kinetics in Kv2.1. *Recept. Chan.* **7**:65–75

Seoh, S.A., Sigg, D., Papazian, D.M., Bezanilla, F. 1996. Voltage-sensing residues in the S2 and S4 segments of the Shaker K$^+$ channel. *Neuron* **16**:1159–1167

Shih, T.M., Goldin, A.L. 1997. Topology of the Shaker potassium channel probed with hydrophilic epitope insertions. *J. Cell Biol.* **136:**1037–1045

Starace, D.M., Stefani, E., Bezanilla, F. 1997. Voltage-dependent proton transport by the voltage sensor of the Shaker K$^+$ channel. *Neuron* **19:**1319–1327

Tiwari-Woodruff, S.K., Schulteis, C.T., Mock, A.F., Papazian, D.M. 1997. Electrostatic interactions between transmembrane segments mediate folding of Shaker K$^+$ channel subunits. *Biophys. J.* **72:**1489–1500

Yusaf, S.P., Wray, D., Sivaprasadarao, A. 1996. Measurement of the movement of the S4 segment during the activation of a voltage-gated potassium channel. *Pfluegers Arch.* **433:**91–97

Zagotta, W.N., Hoshi, T., Aldrich, R.W. 1994. Shaker potassium channel gating. III: Evaluation of kinetic models for activation. *J. Gen. Physiol.* **103:**321–362